

## Si Substrate Suitable for Radiation-Resistant Space Solar Cells

Hideharu MATSUURA\*, Hirofumi IWATA, Sou KAGAMIHARA, Ryohei ISHIHARA, Masahiko KOMEDA, Hideaki IMAI, Masanori KIKUTA, Yuuki INOUE, Tadashi HISAMATSU<sup>1</sup>, Shirou KAWAKITA<sup>2</sup>, Takeshi OHSHIMA<sup>3</sup> and Hisayoshi ITOH<sup>3</sup>

Department of Electronic Engineering and Computer Science, Osaka Electro-Communication University,  
18-8 Hatsu-cho, Neyagawa, Osaka 572-8530, Japan

<sup>1</sup>Sharp Corporation, 492 Minosho-cho, Yamato-Koriyama, Nara 639-1186, Japan

<sup>2</sup>Japan Aerospace Exploration Agency, 2-1-1 Sengen, Tsukuba, Ibaraki 305-8505, Japan

<sup>3</sup>Japan Atomic Energy Agency, 1233 Watanuki-machi, Takasaki, Gunma 370-1292, Japan

(Received May 25, 2005; accepted December 26, 2005; published online April 7, 2006)

Irradiating group-III (B, Al, Ga)-doped Czochralski (CZ)-grown Si substrates as well as B-doped magnetic Czochralski (MCZ)-grown and floating-zone (FZ)-grown Si substrates with 10 MeV protons or 1 MeV electrons, we investigate both the reduction in the hole concentration and the conversion of p type to n type using Hall-effect measurements. In all the 10 Ω cm CZ-Si, the density of each acceptor species is reduced by irradiation, and finally the conversion occurs with 10<sup>17</sup> cm<sup>-2</sup> fluence of 1 MeV electrons or with 2.5 × 10<sup>14</sup> cm<sup>-2</sup> fluence of 10 MeV protons. In 10 Ω cm MCZ-Si and 10 Ω cm FZ-Si, on the other hand, the conversion does not occur under the same conditions. Moreover, the reduction in the hole concentration for the FZ-Si is much less than the others. From these results, it is elucidated that the conversion as well as the reduction in the hole concentration is strongly dependent on the concentration of oxygen in Si, not on the type of acceptor species in Si. Therefore, the p-type FZ-Si substrate is appropriate for radiation-resistant space solar cells such as n<sup>+</sup>/p/p<sup>+</sup> Si solar cells and upcoming III–V tandem solar cells on n<sup>+</sup>/p Si substrates. [DOI: 10.1143/JJAP.45.2648]

KEYWORDS: Si solar cell, space solar cell, proton irradiation, electron irradiation, radiation damage, solar cell, Si

### 1. Introduction

Because solar cells have been major power source of artificial satellites, enhancements in their conversion efficiency ( $\eta$ ) and radiation hardness and the reduction in their weight have been attempted. Until approximately 7 years ago, prime space solar cells were n<sup>+</sup>/p/p<sup>+</sup> Si solar cells. However, a thin III–V compound semiconductor tandem cell with a thick Ge cell (i.e., Ge substrate) has recently replaced Si solar cells. A typical structure of the tandem cell is GaInP (top cell)/GaAs (middle cell)/Ge (bottom cell), where the adjoining cells are electrically connected by a tunnel junction. However, the Ge substrate is heavier, more fragile and more expensive than the Si substrate. Therefore, Si is expected as a bottom cell material. For example, a two-junction cell composed of a top junction with a band gap ( $E_g$ ) of 1.75 eV and a bottom junction with an  $E_g$  of 1.1 eV has a nearly optimal set of band gaps for high-efficiency solar cells, whose  $\eta$  is theoretically estimated as ~37%.<sup>2,3</sup> This indicates that n<sup>+</sup>/p Si is more suitable for a bottom junction than n<sup>+</sup>/p GaAs or n<sup>+</sup>/p Ge. Although InGaP/Si is one of the optimum candidates from the viewpoint of the set of band gaps, this is a lattice-mismatched combination. Recently lattice-matched GaNPAs/Si has been investigated.<sup>3</sup> Moreover, some papers have indicated the superiority of Si solar cells under LILT (low-intensity, low-temperature) conditions, particularly on Mars.<sup>4,5</sup>

Space solar cells are exposed to a lot of protons and electrons with a high energy. Irradiation lowers  $\eta$ . In particular, n<sup>+</sup>/p/p<sup>+</sup> Si solar cells used in the Engineering Test Satellite-VI, which was constructed by the National Space Development Agency of Japan (NASDA) and launched in August 1994, were heavily damaged in the Van Allen radiation belts.<sup>6</sup> This phenomenon is strongly related to a decrease in the hole concentration in the p

substrate and the conversion of p type to n type with irradiation of protons and electrons.<sup>7–22</sup> Here, the acceptor species in the p-type Si substrates was B.

The densities and energy levels of traps have usually been evaluated using deep-level transient spectroscopy (DLTS). From those studies, the origins of traps created by irradiation were investigated.<sup>23–35</sup> Judging from those results, in B-doped p-type Si, Yamaguchi *et al.*<sup>14–19</sup> reported that hole traps with  $E_V + 0.18$  eV and  $E_V + 0.36$  eV and a donorlike defect with  $E_C - 0.18$  eV were mainly introduced by irradiation, which were considered to be a divacancy (V–V), a complex (C<sub>i</sub>–O<sub>i</sub>) of an interstitial C (C<sub>i</sub>) and an interstitial O (O<sub>i</sub>), and a complex (B<sub>i</sub>–O<sub>i</sub>) of an interstitial B (B<sub>i</sub>) and O<sub>i</sub>, respectively, where  $E_V$  is the valence band maximum and  $E_C$  is the conduction band minimum. In Ga-doped p-type Si, they also reported that the generation of the hole trap with  $E_V + 0.36$  eV was strongly suppressed compared with B-doped p-type Si, and the donorlike defect with  $E_C - 0.18$  eV was not detected.<sup>20,21</sup>

From DLTS, however, the quantitative relationship between the hole concentration and the trap densities is far from complete. This is because in the DLTS analysis the following approximation is assumed.<sup>36,37</sup>

$$C(t) = C(\infty) \sqrt{1 - \frac{N_{\text{Trap}}}{N_{\text{Dopant}} + N_{\text{Trap}}} \exp\left(-\frac{t}{\tau_{\text{Trap}}}\right)} \\ \simeq C(\infty) \left[1 - \frac{N_{\text{Trap}}}{2(N_{\text{Dopant}} + N_{\text{Trap}})} \exp\left(-\frac{t}{\tau_{\text{Trap}}}\right)\right] \quad (1)$$

when

$$\frac{N_{\text{Trap}}}{N_{\text{Dopant}} + N_{\text{Trap}}} \ll 1, \quad (2)$$

where  $C(t)$  is the transient capacitance after a reverse bias is applied for a pn diode or a Schottky barrier diode,  $C(\infty)$  is the steady-state capacitance,  $N_{\text{Dopant}}$  is the dopant density,  $N_{\text{Trap}}$  is the trap density, and  $\tau_{\text{Trap}}$  is the time constant

\*E-mail address: matsuura@isc.osakac.ac.jp

corresponding to the trap. As a result, DLTS can only determine the  $N_{\text{Trap}}$  much lower than the  $N_{\text{Dopant}}$ .

Hall-effect measurements provide the temperature dependence of the hole concentration  $p(T)$  in p-type semiconductors. If the densities and energy levels of traps can be directly determined using  $p(T)$ , the relationship between  $p(T)$  and the trap densities can be directly investigated. As one of the analyses, free-carrier concentration spectroscopy (FCCS) has been proposed and tested.<sup>9,11,38–44</sup> From FCCS, the donorlike defect with  $E_C - 0.3$  eV was reported in the type-converted samples,<sup>11</sup> which was different from the donorlike defect with  $E_C - 0.18$  eV from DLTS.<sup>13–21</sup> The result obtained from FCCS is consistent with other reports.<sup>10,24,25,32</sup>

Using group-III (B, Al, Ga)-doped Czochralski (CZ)-grown Si wafers as well as B-doped magnetic Czochralski (MCZ)-grown and floating-zone (FZ)-grown Si wafers, we report on our investigation of the relationship between the generation of hole traps as well as donorlike defects by irradiation and the acceptor species (i.e., B, Al and Ga) in Si, or between the generation of hole traps as well as donorlike defects and the concentration of O ( $C_O$ ) in Si. Furthermore, the dependence of the reduction in  $p(T)$  on the resistivity of B-doped CZ-Si is investigated. To determine the densities and energy levels of hole traps from  $p(T)$ , FCCS is applied here.

## 2. Experimental

The samples measured here were 10  $\Omega$  cm B-doped single-crystalline Si wafers grown by the CZ, MCZ, and FZ methods, and 1  $\Omega$  cm B-doped single-crystalline CZ-Si wafers. From radioactivation analyses,  $C_O$  and the concentration of C ( $C_C$ ) in the wafer were determined as  $8 \times 10^{17}$  and  $1 \times 10^{15}$   $\text{cm}^{-3}$  for the CZ-Si,  $2 \times 10^{17}$  and  $8 \times 10^{15}$   $\text{cm}^{-3}$  for the MCZ-Si, and  $1 \times 10^{15}$  and  $5 \times 10^{15}$   $\text{cm}^{-3}$  for the FZ-Si. 10  $\Omega$  cm Al- and Ga-doped single-crystalline CZ-Si wafers were also measured. The values of  $C_O$  and  $C_C$  were respectively  $5 \times 10^{17}$  and  $8 \times 10^{15}$   $\text{cm}^{-3}$  for the Al-doped CZ-Si, and  $8 \times 10^{17}$  and  $8 \times 10^{15}$   $\text{cm}^{-3}$  for the Ga-doped CZ-Si. The thickness and size of samples for Hall-effect measurements were 220  $\mu\text{m}$  and  $5 \times 5$   $\text{mm}^2$ . After irradiation by 1 MeV electrons or 10 MeV protons at several fluences, Au was evaporated on the four corners of the surface of the sample. Then, the Hall-effect measurement was conducted by the van der Pauw method in a magnetic field of 1.4 T using a modified MMR Technologies' Hall system. The temperature range of the measurement was limited from 85 to 350 K because some defects are likely to be annealed out at  $\sim 400$  K.<sup>12</sup>

## 3. Results

Figure 1 shows the temperature dependence of the majority-carrier concentration for the proton-irradiated 10  $\Omega$  cm B-doped CZ-Si. The diamonds, triangles, squares, and solid circles correspond to the fluences of 0,  $1.0 \times 10^{13}$ ,  $1.0 \times 10^{14}$ , and  $2.5 \times 10^{14}$   $\text{cm}^{-2}$ , respectively. Only the wafer irradiated with  $2.5 \times 10^{14}$   $\text{cm}^{-2}$  fluence showed n-type conduction.

Figure 2 is the temperature dependence of the majority-carrier concentration for the 10  $\Omega$  cm Al-doped CZ-Si proton-irradiated with the fluences of 0,  $1.0 \times 10^{13}$ ,  $1.0 \times 10^{14}$ , and  $2.5 \times 10^{14}$   $\text{cm}^{-2}$ , denoted by  $\diamond$ ,  $\triangle$ ,  $\square$ , and  $\bullet$ , respectively. The conduction of the wafer irradiated with  $2.5 \times 10^{14}$   $\text{cm}^{-2}$  fluence was of the n type.

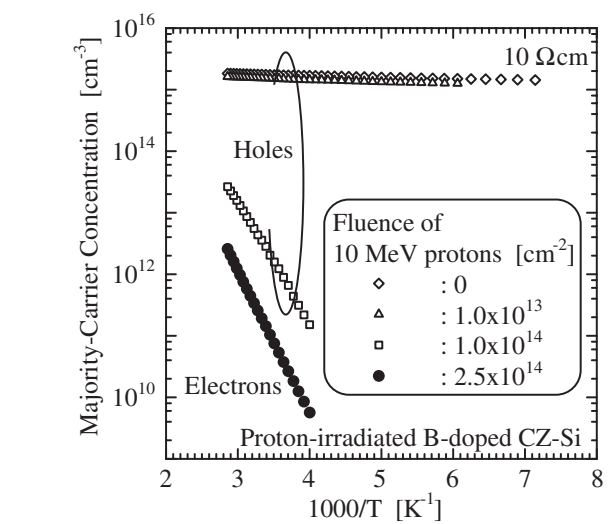


Fig. 1. Temperature dependence of majority-carrier concentration for 10  $\Omega$  cm B-doped CZ-Si irradiated with several fluences of 10 MeV protons.

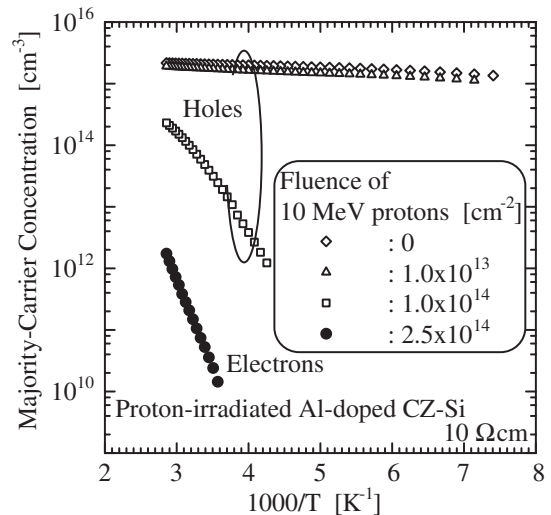


Fig. 2. Temperature dependence of majority-carrier concentration for 10  $\Omega$  cm Al-doped CZ-Si irradiated with several fluences of 10 MeV protons.

Figure 3 depicts the temperature dependence of the majority-carrier concentration for the proton-irradiated 10  $\Omega$  cm Ga-doped CZ-Si. The  $\diamond$ ,  $\triangle$ ,  $\square$ , and  $\bullet$  symbols correspond to the fluences of 0,  $1.0 \times 10^{13}$ ,  $1.0 \times 10^{14}$ , and  $2.5 \times 10^{14}$   $\text{cm}^{-2}$ , respectively. The majority carriers in the wafer irradiated with  $2.5 \times 10^{14}$   $\text{cm}^{-2}$  fluence were electrons.

With irradiation at  $2.5 \times 10^{14}$   $\text{cm}^{-2}$  fluence, the type conversion occurred in the 10  $\Omega$  cm CZ-Si with any acceptor species (i.e., B, Al and Ga). Furthermore, the electron concentrations in the type-converted samples were similar. Therefore, the conversion is independent of the acceptor species in Si.

According to the literature,<sup>11,12,17,19–21</sup> the type conversion was considered to result from not only the creation of

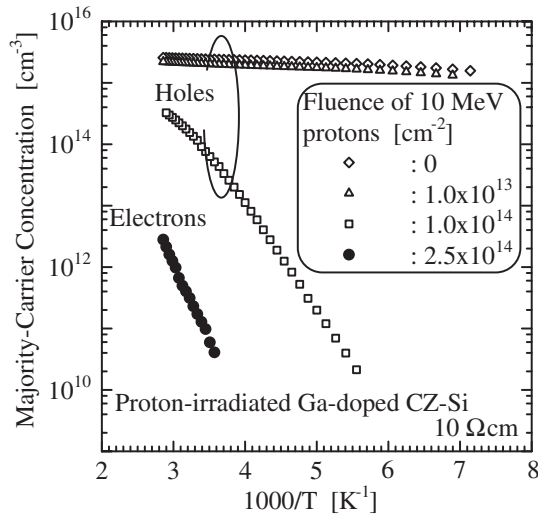


Fig. 3. Temperature dependence of majority-carrier concentration for 10 Ωcm Ga-doped CZ-Si irradiated with several fluences of 10 MeV protons.

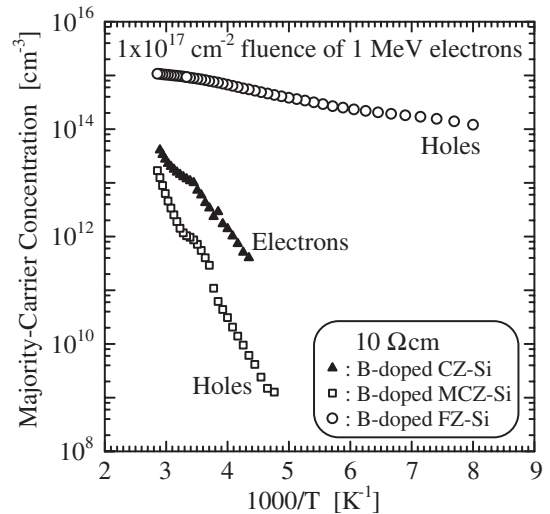


Fig. 5. Temperature dependence of majority-carrier concentration for 10 Ωcm B-doped CZ-, MCZ-, and FZ-Si irradiated with  $1.0 \times 10^{17} \text{ cm}^{-2}$  fluence of 1 MeV electrons.

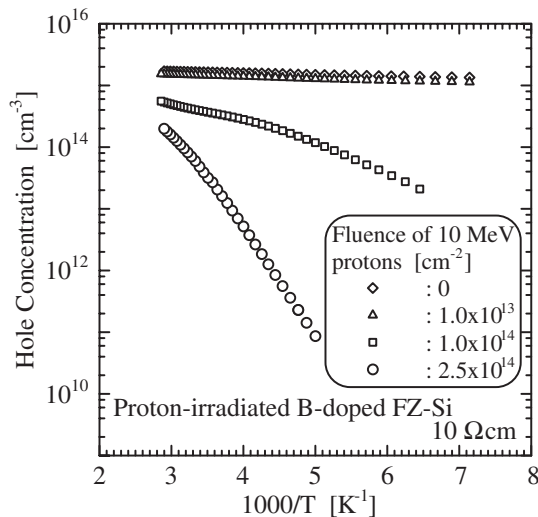


Fig. 4. Temperature dependence of hole concentration for 10 Ωcm B-doped FZ-Si irradiated with several fluences of 10 MeV protons.

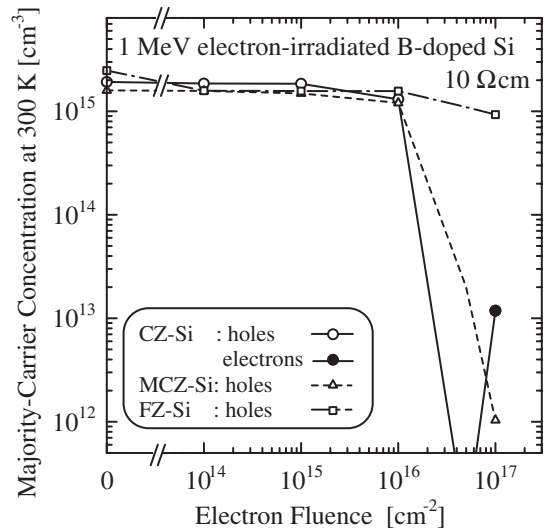


Fig. 6. Dependence of majority-carrier concentration at 300 K on fluence of 1 MeV electrons for 10 Ωcm B-doped CZ-, MCZ-, and FZ-Si.

hole traps but also the creation of donorlike defects that are considered to be  $B_i-O_i$ . However, the conversion occurred in the Al- or Ga-doped Si, suggesting that the donorlike defect induced by irradiation may be a complex of  $O_i$  and an interstitial group-III atom. Therefore, we next investigate if the donorlike defect is related to O in Si.

Figure 4 shows the  $p(T)$  for the 10 Ωcm B-doped FZ-Si irradiated with several fluences of 10 MeV protons. Here, the  $C_0$  in the FZ-Si is  $\sim 800$  less than the  $C_0$  in the CZ-Si. The  $\diamond$ ,  $\triangle$ ,  $\square$ , and  $\circ$  symbols correspond to the fluences of 0,  $1.0 \times 10^{13}$ ,  $1.0 \times 10^{14}$ , and  $2.5 \times 10^{14} \text{ cm}^{-2}$ , respectively. The reduction in  $p(T)$  with irradiation at  $1.0 \times 10^{14} \text{ cm}^{-2}$  fluence was much less than in the 10 Ωcm CZ-Si. Even with irradiation at  $2.5 \times 10^{14} \text{ cm}^{-2}$  fluence, moreover, the type conversion did not occur. The main difference between the FZ-Si and CZ-Si is the difference in  $C_0$ . As the  $C_0$  in Si is lower, the formation of the donorlike defect with irradiation becomes suppressed. Therefore, it is clear that O is related to

the donorlike defect.

Figure 5 is the temperature dependence of the majority-carrier concentration for the 10 Ωcm B-doped CZ-, MCZ-, or FZ-Si irradiated with  $1.0 \times 10^{17} \text{ cm}^{-2}$  fluence of 1 MeV electrons. The solid triangles represent the temperature dependence of the electron concentration,  $n(T)$ , for the 10 Ωcm B-doped CZ-Si, whereas  $\square$  and  $\circ$  represent the  $p(T)$  in the 10 Ωcm B-doped MCZ- and FZ-Si. Although the  $p(T)$  in the 10 Ωcm MCZ-Si was markedly reduced by irradiation with  $1.0 \times 10^{17} \text{ cm}^{-2}$  fluence of 1 MeV electrons, its majority carriers remained holes. Furthermore, the  $p(T)$  in the 10 Ωcm FZ-Si decreased slightly.

Figure 6 shows the dependence of the majority-carrier concentration at 300 K on the fluence of 1 MeV electrons for the 10 Ωcm B-doped CZ-, MCZ-, and FZ-Si. The  $p(T)$  in the 10 Ωcm CZ-, MCZ-, and FZ-Si are denoted by  $\diamond$ ,  $\triangle$ , and  $\square$ , respectively, whereas the  $n(T)$  for the 10 Ωcm CZ-Si is denoted by  $\bullet$ . The large decrease in  $p(T)$  or the type

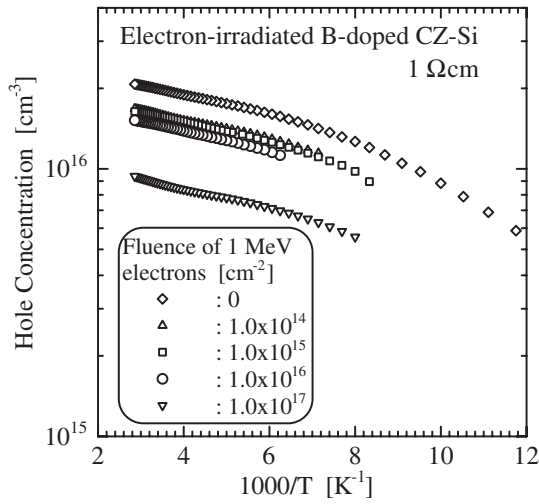


Fig. 7. Temperature dependence of hole concentration for 1 Ωcm B-doped CZ-Si irradiated with several fluences of 1 MeV electrons.

conversion with irradiation is found to occur at above  $1.0 \times 10^{16} \text{ cm}^{-2}$  fluence in the 10 Ω cm CZ- and MCZ-Si, while the  $p(T)$  is reduced slightly in the 10 Ω cm FZ-Si.

Similar to the proton irradiation, the type conversion occurred in the 10 Ω cm Al- or Ga-doped CZ-Si with irradiation by 1 MeV electrons at  $1.0 \times 10^{17} \text{ cm}^{-2}$  fluence. Therefore, the 10 Ω cm FZ-Si is found to be more radiation resistant than the other samples.

Figure 7 shows the  $p(T)$  in the 1 Ω cm B-doped CZ-Si irradiated with several fluences of 1 MeV electrons. The  $\diamond$ ,  $\triangle$ ,  $\square$ ,  $\circ$ , and  $\nabla$  symbols correspond to the fluences of 0,  $1.0 \times 10^{14}$ ,  $1.0 \times 10^{15}$ ,  $1.0 \times 10^{16}$ , and  $1.0 \times 10^{17} \text{ cm}^{-2}$ , respectively. Although the type conversion in the 1 Ω cm B-doped CZ-Si did not occur with  $1.0 \times 10^{17} \text{ cm}^{-2}$  fluence because of its higher acceptor density, the decrease in the  $p(T)$  in the 1 Ω cm B-doped CZ-Si was much larger than that in the 10 Ω cm B-doped CZ-Si with irradiation at the same fluence. Since the reduction in the hole concentration results from the generation of defects that reduce the electron diffusion length, 10 Ω cm p-type Si is more suitable for the substrate of space solar cells than 1 Ω cm p-type Si.

In the following, the reduction in the acceptor density ( $N_A$ ) as well as the increase in hole-trap densities induced by irradiation is investigated from  $p(T)$  determined using FCCS.

## 4. FCCS

### 4.1 Basic concept

DLTS,<sup>36)</sup> isothermal capacitance transient spectroscopy (ICTS),<sup>45)</sup> and some methods<sup>46,47)</sup> can uniquely determine the densities and energy levels of traps in semiconductors or insulators, because each peak in the signal corresponds one-to-one to a trap. For example, the ICTS signal is defined as  $S(t) \equiv tdC(t)^2/dt$ . Since  $S(t)$  is theoretically described as the sum of  $N_i e_i t \exp(-e_i t)$ , it has a peak value of  $N_i \exp(-1)$  at a peak time of  $t_{\text{peak}i} = 1/e_i$ . Here,  $N_i$  and  $e_i$  are the density and emission rate of an  $i$ th trap. Therefore, the function of  $N_i e_i t \exp(-e_i t)$  plays an important role in the ICTS analysis.

DLTS is powerful methods for investigating defects

and impurities with deep energy levels. As a consequence, a lot of results related to the radiation damages of Si were reported from studies of DLTS. To accurately determine their densities and energy levels, however, their densities should be much less than the dopant density.<sup>37)</sup> Therefore, the impurities and defects that affect the majority-carrier concentration should be investigated using the data obtained from Hall-effect measurements.<sup>9)</sup>

To analyze the  $p(T)$ , we have introduced a function theoretically described as the sum of  $N_{\text{TH}i} \exp(-\Delta E_{\text{TH}i}/kT)/kT$ ,<sup>38)</sup> where  $k$  is the Boltzmann constant,  $N_{\text{TH}i}$  and  $\Delta E_{\text{TH}i}$  are the density and energy level of an  $i$ th hole trap, and  $\Delta E_{\text{TH}i}$  is measured from  $E_V$ . The function of  $N_{\text{TH}i} \exp(-\Delta E_{\text{TH}i}/kT)/kT$  has a peak at  $T_{\text{peak}i} = \Delta E_{\text{TH}i}/k$ , which does not apply to all the hole traps in the temperature range of the measurement. If you introduce a function in which a peak appears at  $T_{\text{peak}i} = (\Delta E_{\text{TH}i} - E_{\text{ref}})/k$ , you can shift the peak temperature to the measurement temperature range by changing the parameter  $E_{\text{ref}}$ . This indicates that you can determine  $N_{\text{TH}i}$  and  $\Delta E_{\text{TH}i}$  in a wide range of hole-trap levels even within a limited measurement temperature range. Therefore, the function to be evaluated should be approximately described as the sum of  $N_{\text{TH}i} \exp[-(\Delta E_{\text{TH}i} - E_{\text{ref}})/kT]/kT$ . It should be noted that the values of  $N_{\text{TH}i}$  and  $\Delta E_{\text{TH}i}$  determined by this method are independent of  $E_{\text{ref}}$ .

### 4.2 Theoretical consideration

In the following, we assume a p-type semiconductor with one acceptor species ( $N_A$ : acceptor density and  $\Delta E_A$ : acceptor level),  $l$  types of hole traps, and a total donor density ( $N_D$ ), where hole traps are positively charged when they capture holes. From the charge neutrality condition,  $p(T)$  can be written as<sup>48)</sup>

$$p(T) = N_A f_{\text{FD}}(\Delta E_A) - \sum_{i=1}^l N_{\text{TH}i} [1 - f_{\text{FD}}(\Delta E_{\text{TH}i})] - N_D \quad (3)$$

in the temperature range in which  $n(T)$  is much less than  $p(T)$ , where  $f_{\text{FD}}(\Delta E)$  is the Fermi-Dirac distribution function, which is given by<sup>48)</sup>

$$f_{\text{FD}}(\Delta E) = \frac{1}{1 + g_A \exp\left(-\frac{\Delta E_{\text{F}}(T) - \Delta E}{kT}\right)} \quad (4)$$

Here,  $\Delta E_{\text{F}}(T)$  is the Fermi level measured from  $E_V$  at  $T$ ,  $g_A$  is the acceptor degeneracy factor of 4, and  $\Delta E$  represents  $\Delta E_A$  or  $\Delta E_{\text{TH}i}$ .

On the other hand, using the effective density of states  $N_V(T)$  in the valence band,  $p(T)$  is expressed as<sup>48)</sup>

$$p(T) = N_V(T) \exp\left(-\frac{\Delta E_{\text{F}}(T)}{kT}\right), \quad (5)$$

where

$$N_V(T) = N_{V0} k^{3/2} T^{3/2}, \quad (6)$$

$$N_{V0} = 2 \left( \frac{2\pi m_h^*}{h^2} \right)^{3/2}, \quad (7)$$

$m_h^*$  is the hole effective mass, and  $h$  is Planck's constant.

It is clear from the following discussion that a favorable function is defined as

$$H(T, E_{\text{ref}}) \equiv \frac{p(T)^2}{(kT)^{5/2}} \exp\left(\frac{E_{\text{ref}}}{kT}\right). \quad (8)$$

Substituting eq. (3) for one of the  $p(T)$  in eq. (8) and substituting eq. (5) for the other  $p(T)$  in eq. (8) yield

$$H(T, E_{\text{ref}}) = \frac{N_A}{kT} \exp\left(-\frac{\Delta E_A - E_{\text{ref}}}{kT}\right) I(\Delta E_A) + \sum_{i=1}^l \frac{N_{\text{TH}i}}{kT} \exp\left(-\frac{\Delta E_{\text{TH}i} - E_{\text{ref}}}{kT}\right) I(\Delta E_{\text{TH}i}) - \frac{N_{\text{comp}} N_{\text{V}0}}{kT} \exp\left(\frac{E_{\text{ref}} - \Delta E_{\text{F}}(T)}{kT}\right), \quad (9)$$

where

$$I(\Delta E) = N_{\text{V}0} \exp\left(\frac{\Delta E - \Delta E_{\text{F}}(T)}{kT}\right) f_{\text{FD}}(\Delta E) \quad (10)$$

and

$$N_{\text{comp}} = N_{\text{D}} + \sum_{i=1}^l N_{\text{TH}i}. \quad (11)$$

The function

$$\frac{N}{kT} \exp\left(-\frac{\Delta E - E_{\text{ref}}}{kT}\right) \quad (12)$$

in eq. (9) has a peak value of  $N \exp(-1)/kT_{\text{peak}}$  at the peak temperature

$$T_{\text{peak}} = \frac{\Delta E - E_{\text{ref}}}{k}, \quad (13)$$

where  $N$  represents  $N_A$  or  $N_{\text{TH}i}$ . As is clear from eq. (13), the  $E_{\text{ref}}$  can shift the peak of  $H(T, E_{\text{ref}})$  within the temperature range of the measurement. Although the actual  $T_{\text{peak}}$  of  $H(T, E_{\text{ref}})$  is slightly different from the value calculated by eq. (13) due to the temperature dependence of  $I(\Delta E)$ , you can easily determine the accurate density and energy level from each peak of the experimental  $H(T, E_{\text{ref}})$ , using a personal computer. The Windows application software for FCCS can be downloaded for free at our web site (<http://www.osakac.ac.jp/labs/matsuura/>).

#### 4.3 Determination of densities and energy levels

The following shows how to determine the densities and energy levels of hole traps for the 10 Ω cm B-doped FZ-Si irradiated with  $1.0 \times 10^{13} \text{ cm}^{-2}$  fluence of 10 MeV protons from FCCS. The open and solid triangles in Fig. 8 represent the  $p(T)$  and the  $H(T, E_{\text{ref}})$  with an  $E_{\text{ref}}$  of  $-2.5 \times 10^{-2} \text{ eV}$ , where the FCCS signal was calculated from eq. (8). Since this FCCS signal has one peak and one shoulder, this substrate includes at least two types of hole trap. The peak temperature and peak value of the FCCS signal were 161 K and  $1.0 \times 10^{34} \text{ cm}^{-6} \text{ eV}^{-2.5}$ , respectively. From this peak, the energy level ( $\Delta E_{\text{TH}1}$ ) and density ( $N_{\text{TH}1}$ ) of the corresponding hole trap were determined as 98 meV and  $2.0 \times 10^{14} \text{ cm}^{-3}$ , respectively.

To investigate other hole traps corresponding to the shoulder, the FCCS signal of  $H2(T, E_{\text{ref}})$ , in which the influence of the previously determined hole trap is removed, is calculated using the following equation. It is clear from

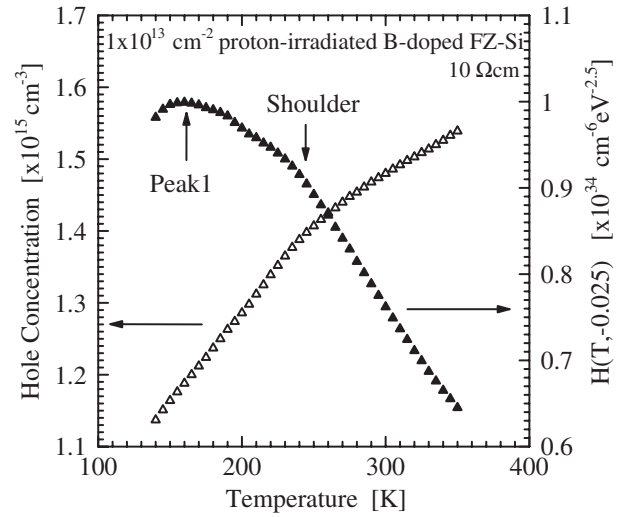


Fig. 8. Temperature dependence of hole concentration or FCCS signal for  $1.0 \times 10^{13} \text{ cm}^{-2}$  proton-irradiated 10 Ω cm B-doped FZ-Si.

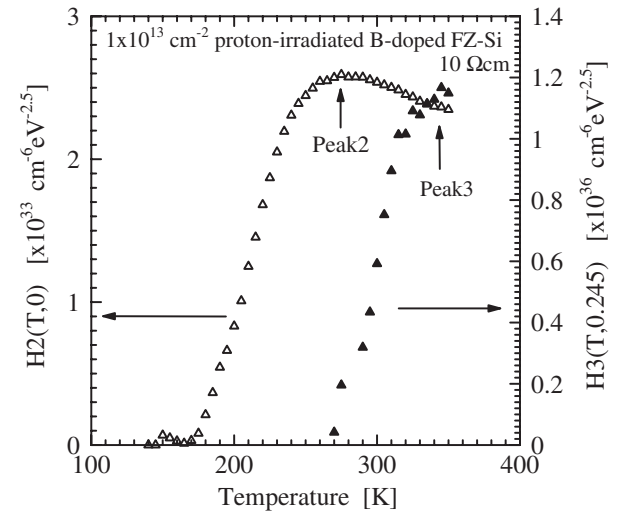


Fig. 9. FCCS signals for  $1.0 \times 10^{13} \text{ cm}^{-2}$  proton-irradiated 10 Ω cm B-doped FZ-Si.

eqs. (8) and (9) that

$$H2(T, E_{\text{ref}}) = \frac{p(T)^2}{(kT)^{5/2}} \exp\left(\frac{E_{\text{ref}}}{kT}\right) - \frac{N_{\text{TH}1}}{kT} \exp\left(-\frac{\Delta E_{\text{TH}1} - E_{\text{ref}}}{kT}\right) I(\Delta E_{\text{TH}1}) \quad (14)$$

is not influenced by the hole trap with  $\Delta E_{\text{TH}1}$ .

The open triangles in Fig. 9 represent  $H2(T, E_{\text{ref}})$  with an  $E_{\text{ref}}$  of 0 eV. Using the peak temperature of 278 K and the peak value of  $2.6 \times 10^{33} \text{ cm}^{-6} \text{ eV}^{-2.5}$ , the hole-trap level ( $\Delta E_{\text{TH}2}$ ) and density ( $N_{\text{TH}2}$ ) were determined to be 157 meV and  $2.2 \times 10^{14} \text{ cm}^{-3}$ , respectively.

The FCCS signal of  $H3(T, E_{\text{ref}})$ , in which the influence of two hole traps previously determined is removed, is calculated by

$$H3(T, E_{\text{ref}}) = \frac{p(T)^2}{(kT)^{5/2}} \exp\left(\frac{E_{\text{ref}}}{kT}\right) - \sum_{i=1}^2 \frac{N_{\text{TH}i}}{kT} \exp\left(-\frac{\Delta E_{\text{TH}i} - E_{\text{ref}}}{kT}\right) I(\Delta E_{\text{TH}i}). \quad (15)$$

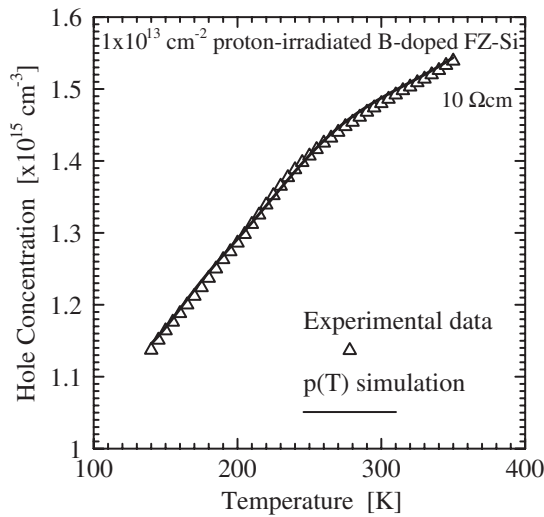


Fig. 10. Experimental and simulated  $p(T)$  for  $1.0 \times 10^{13} \text{ cm}^{-2}$  proton-irradiated  $10 \Omega \text{ cm}$  B-doped FZ-Si.

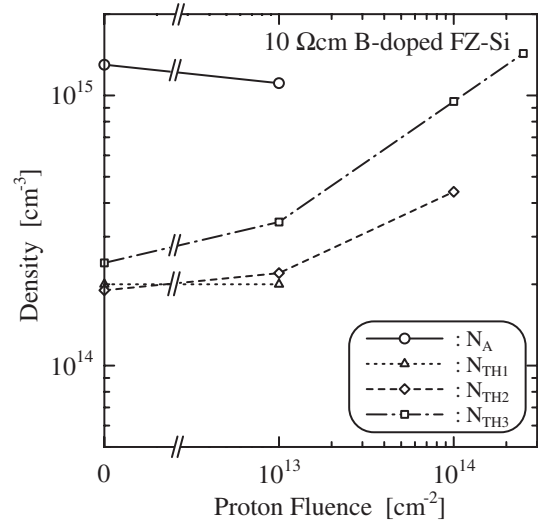


Fig. 11. Dependence of  $N_A$  or  $N_{THi}$  for  $10 \Omega \text{ cm}$  B-doped FZ-Si on fluence of 10 MeV protons.

The solid triangles in Fig. 9 represent  $H3(T, E_{ref})$  with an  $E_{ref}$  of 0.245 eV. Using the peak temperature of 339 K and the peak value of  $1.2 \times 10^{36} \text{ cm}^{-6} \text{ eV}^{-2.5}$ , the hole-trap level ( $\Delta E_{TH3}$ ) and density ( $N_{TH3}$ ) were determined as 299 meV and  $3.4 \times 10^{14} \text{ cm}^{-3}$ , respectively.

The FCCS signal of  $H4(T, E_{ref})$ , in which the influence of three hole traps previously determined was removed, was calculated. However, the  $H4(T, E_{ref})$  was nearly zero, indicating that this FZ-Si contains three types of hole trap mainly affecting  $p(T)$  in the measurement temperature range. Finally, the value of  $N_A - N_{comp}$  was determined as  $1.11 \times 10^{15} \text{ cm}^{-3}$ , respectively.

To verify the values obtained by FCCS,  $p(T)$  was simulated using eqs. (3) and (5). The triangles in Fig. 10 represent the experimental  $p(T)$ , and the solid line represents the  $p(T)$  simulation. Since the solid line is in good agreement with  $\Delta$ , the values determined by FCCS are reliable.<sup>49)</sup>

In the same way as illustrated for this sample, the densities and energy levels for the other samples were determined.

### 5. Discussion

The densities and energy levels of hole traps for the  $10 \Omega \text{ cm}$  B-doped FZ-Si with 10 MeV protons are listed in Table I. The values of the lowest  $\Delta E_F(T)$  in the temperature range of the measurement were 95, 97, 162, and 310 meV for the samples irradiated with the fluences of 0,  $1.0 \times 10^{13}$ ,

$1.0 \times 10^{14}$ , and  $2.5 \times 10^{14} \text{ cm}^{-2}$ , respectively. Since the  $\Delta E_A$  of B in Si is  $\sim 45 \text{ meV}$ , B acceptors were completely ionized at the lowest measurement temperature, indicating that  $\Delta E_A$  could not be determined in this measurement temperature range. Because in the case of  $1.0 \times 10^{14} \text{ cm}^{-2}$  fluence the hole traps with  $\Delta E_{TH1}$  were not filled with holes at all in the measurement temperature range, the values of  $\Delta E_{TH1}$  and  $N_{TH1}$  could not be evaluated. For the same reason, the values of  $\Delta E_{TH1}$ ,  $N_{TH1}$ ,  $\Delta E_{TH2}$ , and  $N_{TH2}$  could not be estimated in the sample irradiated with the  $2.5 \times 10^{14} \text{ cm}^{-2}$  fluence.

Figure 11 shows the dependencies of acceptor density and hole-trap densities on proton fluence. The values of  $N_{TH2}$  and  $N_{TH3}$  increase clearly. Moreover, the  $N_{TH3}$  of the sample irradiated with  $2.5 \times 10^{14} \text{ cm}^{-2}$  exceeds the  $N_A$  of the unirradiated sample. Because the density and energy level of the hole trap with a density higher than the acceptor density can be determined from FCCS, FCCS is superior to DLTS from the viewpoint of the evaluation of traps with high densities.

Irradiation introduces a vacancy (V), an interstitial Si ( $\text{Si}_i$ ), and  $\text{B}_i$  in B-doped Si. From Fourier-transform infrared spectroscopy at low temperatures, the density of a substitutional B ( $\text{B}_s$ ), which acts as an acceptor, is reported to decrease with increasing fluence,<sup>11,50)</sup> indicating that  $\text{B}_i$  is created by irradiation. In Fig. 11, furthermore, the values of  $N_{TH2}$  and  $N_{TH3}$  increase with fluence. At  $1.0 \times 10^{14}$  and

Table I. Densities and energy levels determined by FCCS for 10 MeV proton-irradiated  $10 \Omega \text{ cm}$  B-doped FZ-Si.

Proton fluence ( $\text{cm}^{-2}$ )	0	$1 \times 10^{13}$	$1 \times 10^{14}$	$2.5 \times 10^{14}$	Origins
$N_A - N_{comp}$ ( $\times 10^{15} \text{ cm}^{-3}$ )	1.30	1.11	—	—	
$\Delta E_{TH1}$ (meV)	91	99	—	—	$\text{Fe}_i\text{-B}_s$ ?
$N_{TH1}$ ( $\times 10^{15} \text{ cm}^{-3}$ )	0.20	0.20	—	—	
$\Delta E_{TH2}$ (meV)	150	157	179	—	V-V
$N_{TH2}$ ( $\times 10^{15} \text{ cm}^{-3}$ )	0.19	0.22	0.44	—	
$\Delta E_{TH3}$ (meV)	281	299	315	319	$\text{C}_i\text{-C}_s$ or $\text{C}_i\text{-O}_i$
$N_{TH3}$ ( $\times 10^{15} \text{ cm}^{-3}$ )	0.24	0.34	0.95	1.43	
$N_{comp} - N_A$ ( $\times 10^{15} \text{ cm}^{-3}$ )	—	—	0.01	0.19	

Table II. Densities and energy levels determined by FCCS for 10 MeV proton-irradiated 10 Ω cm B-, Al-, and Ga-doped CZ-Si.

Dopant	B		Al		Ga		Origins
	Proton fluence (cm <sup>-2</sup> )	0	1 × 10 <sup>13</sup>	0	1 × 10 <sup>13</sup>	0	
ΔE <sub>A</sub> (meV)	—	—	67	69	71	74	group-III
N <sub>A</sub> (×10 <sup>15</sup> cm <sup>-3</sup> )	1.44	1.24	1.98	1.58	2.39	1.95	
ΔE <sub>TH1</sub> (meV)	112	121	—	—	—	—	Fe <sub>i</sub> -B <sub>s</sub> ?
N <sub>TH1</sub> (×10 <sup>15</sup> cm <sup>-3</sup> )	0.26	0.22	—	—	—	—	
ΔE <sub>TH2</sub> (meV)	201	198	180	180	201	203	V-V
N <sub>TH2</sub> (×10 <sup>15</sup> cm <sup>-3</sup> )	0.20	0.23	0.26	0.41	0.33	0.41	

Table III. Densities and energy levels determined by FCCS for 1 MeV electron-irradiated 1 Ω cm B-doped CZ-Si.

Electron fluence (cm <sup>-2</sup> )	0	1.0 × 10 <sup>14</sup>	1.0 × 10 <sup>15</sup>	1.0 × 10 <sup>16</sup>	1.0 × 10 <sup>17</sup>	Origins
	ΔE <sub>A</sub> (meV)	38	41	41	46	
N <sub>A</sub> (×10 <sup>16</sup> cm <sup>-3</sup> )	1.94	1.55	1.52	1.44	0.84	
ΔE <sub>TH1</sub> (meV)	130	138	121	137	157	Fe <sub>i</sub> -B <sub>s</sub> ?
N <sub>TH1</sub> (×10 <sup>16</sup> cm <sup>-3</sup> )	0.24	0.23	0.18	0.15	0.16	

2.5 × 10<sup>14</sup> cm<sup>-2</sup> fluences, therefore, N<sub>comp</sub> becomes larger than N<sub>A</sub>, as shown in Table I.

Table II shows the densities and energy levels determined by FCCS for the 10 MeV proton-irradiated 10 Ω cm B-, Al-, and Ga-doped CZ-Si. Since the ΔE<sub>A</sub> of Al or Ga in Si is deeper than the ΔE<sub>A</sub> of B in Si, the values of ΔE<sub>A</sub> and N<sub>A</sub> could be determined in the temperature range of the measurement. N<sub>A</sub> clearly decreases due to irradiation, whereas N<sub>TH2</sub> increases with irradiation in all the CZ-Si wafers. Since the hole trap with ΔE<sub>TH1</sub> was not detected in the Al- and Ga-doped CZ-Si, it might be related to B.

Table III shows the densities and energy levels determined by FCCS for the electron-irradiated 1 Ω cm B-doped CZ-Si. The density of B acceptors decreases clearly with increasing electron fluence, and N<sub>TH1</sub> decreases slightly.

Compared with Table I, the deeper hole traps are not shown in Tables II and III, although these defects should exist in CZ-Si. This is because the measurement temperature range was limited under 350 K to avoid annealing out some defects.<sup>12)</sup> That is, the Fermi level at the highest measurement temperature was still shallower than the ΔE<sub>TH2</sub> for the 1 Ω cm CZ-Si or the ΔE<sub>TH3</sub> for the 10 Ω cm CZ-Si.

From DLTS, the energy level of V-V was reported to be E<sub>V</sub> + 0.18 eV by Yamaguchi *et al.*,<sup>14-19)</sup> and E<sub>V</sub> + 0.23 eV by Mooney,<sup>25)</sup> which is in good agreement with the hole trap with the ΔE<sub>TH2</sub> observed here. Furthermore, the V-V density was reported to increase with fluence, which is consistent with the finding that N<sub>TH2</sub> increases with proton fluence. Therefore, the origin of the hole trap with ΔE<sub>TH2</sub> is assigned to V-V.

The energy level of the dominant defect introduced with irradiation was reported to be E<sub>V</sub> + 0.33 ~ 0.36 eV.<sup>14-19,23,35)</sup> Trauwaert *et al.*<sup>35)</sup> reported that those defects were considered to be C<sub>i</sub>-O<sub>i</sub> for a high C<sub>O</sub>, and C<sub>i</sub>-C<sub>s</sub> for a low C<sub>O</sub>. Since it is clear from Fig. 11 that the hole trap with ΔE<sub>TH3</sub> is the dominant defect induced with irradiation, the possible origin of the hole trap with ΔE<sub>TH3</sub> is C<sub>i</sub>-C<sub>s</sub> or C<sub>i</sub>-O<sub>i</sub>.

Song *et al.*<sup>31)</sup> reported that the hole trap with E<sub>V</sub> + 0.09 eV was not observed in irradiated samples while it appeared

after annealing above 340 K, suggesting that it is not the hole trap with ΔE<sub>TH1</sub>. N<sub>TH1</sub> is unchanged or slightly decreased with fluence, which is quite different from the fluence dependence of N<sub>TH2</sub> or N<sub>TH3</sub>. The hole trap with ΔE<sub>TH1</sub> is observed only in the B-doped Si. As is clear from Tables I-III, the ratio of N<sub>TH1</sub> to N<sub>A</sub> of the unirradiated B-doped Si is ~15%. These findings may suggest that this hole trap is a complex of B<sub>s</sub> and some contaminated impurity or a complex of B<sub>s</sub> and some defect. According to the literature,<sup>51,52)</sup> one of the possible origins of the hole trap with ΔE<sub>TH1</sub> is a complex (Fe<sub>i</sub>-B<sub>s</sub>) of B<sub>s</sub> and an interstitial Fe (Fe<sub>i</sub>) whose energy level is ~100 meV.

From the analyses of p(T), the hole traps clearly exist even in unirradiated Si. From DLTS, on the other hand, they were not found in unirradiated Si, and the hole traps corresponding to ΔE<sub>TH2</sub> and ΔE<sub>TH3</sub> were formed by irradiation.<sup>17)</sup> Unfortunately, it is not clear whether the origins of these hole traps observed from p(T) for unirradiated Si are the same as those determined from DLTS in irradiated Si. Further research in this area is in progress.

## 6. Conclusions

With irradiation by 10 MeV protons at 2.5 × 10<sup>14</sup> cm<sup>-2</sup> fluence or by 1 MeV electrons at 1.0 × 10<sup>17</sup> cm<sup>-2</sup> fluence, the conduction of 10 Ω cm B-, Al-, and Ga-doped CZ-Si changed from the p type to the n type. Under the same conditions, on the other hand, the conduction of 10 Ω cm B-doped MCZ- and FZ-Si remained the p type, and the decrease in the p(T) of the FZ-Si was considerably lower, suggesting that the donorlike defect is related to O.

From FCCS, the densities of the hole traps with E<sub>V</sub> + ~0.2 eV and E<sub>V</sub> + ~0.3 eV were found to increase with increasing fluence of 10 MeV protons or 1 MeV electrons. Compared with the results from DLTS, the hole trap with E<sub>V</sub> + ~0.2 eV was assigned to V-V and the hole trap with E<sub>V</sub> + ~0.3 eV was considered to be C<sub>i</sub>-C<sub>s</sub> or C<sub>i</sub>-O<sub>i</sub>. The hole trap with E<sub>V</sub> + ~0.1 eV was detected only in B-doped Si, and unchanged or slightly decreased with irradiation. This may be Fe<sub>i</sub>-B<sub>s</sub>. Moreover, FCCS could determine the density and energy level of the hole trap with

a higher density than the acceptor density, different from DLTS.

The density of the acceptor species (substitutional B, Al, or Ga) has been found to decrease with increasing fluence. Finally, FZ-Si was elucidated to be the most radiation-resistant Si substrate from the viewpoint of the preservation of  $p(T)$ .

### Acknowledgments

The authors would like to thank O. Anzawa, a former researcher of NASDA for preparing the samples, and S. Matsuda of Japan Aerospace Exploration Agency for giving us the opportunity to carry out this work. This work was partially supported by the Academic Frontier Promotion Projects of the Ministry of Education, Culture, Sports, Science and Technology 1998–2002 and 2003–2008.

- 1) T. Soga, T. Kato, M. Yang, M. Umeno and T. Jimbo: *J. Appl. Phys.* **78** (1995) 4196.
- 2) J. C. C. Fan, B.-Y. Tsaur and B. J. Palm: Proc. 16th IEEE Photovoltaic Specialists Conf., New York, 1982, p. 692.
- 3) J. F. Geisz and D. J. Friedman: Proc. 29th IEEE Photovoltaic Specialists Conf., New Orleans, 2002, p. 864.
- 4) G. A. Landis: 2nd World Conf. & Exhib. Photovoltaic Solar Energy Conversion, Vienna, 1998, p. 3695.
- 5) P. M. Stella, G. L. Davis, R. L. Mueller, D. D. Krut, D. Brinker and D. A. Scheiman: Proc. 28th IEEE Photovoltaic Specialists Conf., Anchorage, 2000, p. 1354.
- 6) H. Kitahara, S. Tanaka, Y. Kanamori and T. Itoh: 46th Int. Astronautical Congr., Oslo, 1995, p. 1.
- 7) T. Hisamatsu, O. Kawasaki, S. Matsuda, T. Nakao and Y. Wakow: *Sol. Energy Mater. Sol. Cells* **50** (1998) 331.
- 8) M. Yamaguchi, S. J. Taylor, M. Yang, S. Matsuda, O. Kawasaki and T. Hisamatsu: *Jpn. J. Appl. Phys.* **35** (1996) 3918.
- 9) H. Matsuura, Y. Uchida, T. Hisamatsu and S. Matsuda: *Jpn. J. Appl. Phys.* **37** (1998) 6034.
- 10) T. Hisamatsu, H. Okamoto, N. Shiono, T. Aburaya and S. Matsuda: 11th Int. Photovoltaic Science and Engineering Conf., Sapporo, 1999, p. 159.
- 11) H. Matsuura, Y. Uchida, N. Nagai, T. Hisamatsu, T. Aburaya and S. Matsuda: *Appl. Phys. Lett.* **76** (2000) 2092.
- 12) H. Matsuura, T. Ishida, T. Kirihata, O. Anzawa and S. Matsuda: *Jpn. J. Appl. Phys.* **42** (2003) 5187.
- 13) S. J. Taylor, M. Yamaguchi, M. Yang, M. Imaizumi, S. Matsuda, O. Kawasaki and T. Hisamatsu: *Appl. Phys. Lett.* **70** (1997) 2165.
- 14) S. J. Taylor, M. Yamaguchi, S. Matsuda, T. Hisamatsu and O. Kawasaki: *J. Appl. Phys.* **82** (1997) 3239.
- 15) T. Yamaguchi, S. J. Taylor, S. Watanabe, K. Ando, M. Yamaguchi, T. Hisamatsu and S. Matsuda: *Appl. Phys. Lett.* **72** (1998) 1226.
- 16) S. J. Taylor, M. Yamaguchi, T. Yamaguchi, S. Watanabe, K. Ando, S. Matsuda, T. Hisamatsu and S. I. Kim: *J. Appl. Phys.* **83** (1998) 4620.
- 17) M. Yamaguchi, A. Khan, S. Taylor, K. Ando, T. Yamaguchi, S. Matsuda and T. Aburaya: *J. Appl. Phys.* **86** (1999) 217.
- 18) A. Khan, M. Yamaguchi, S. J. Taylor, T. Hisamatsu and S. Matsuda: *Jpn. J. Appl. Phys.* **38** (1999) 2679.
- 19) A. Khan, M. Yamaguchi, T. Hisamatsu and S. Matsuda: *J. Appl. Phys.* **87** (2000) 2162.
- 20) A. Khan, M. Yamaguchi, Y. Ohshita, N. Dharmarasu, K. Araki, T. Abe, H. Itoh, T. Ohshima, M. Imaizumi and S. Matsuda: *J. Appl. Phys.* **90** (2001) 1170.
- 21) M. Yamaguchi, A. Khan, T. K. Vu, Y. Ohshima and T. Abe: *Physica B* **340–342** (2003) 596.
- 22) H. Amekura, N. Kishimoto and K. Kono: *J. Appl. Phys.* **84** (1998) 4834.
- 23) L. C. Kimerling: *IEEE Trans. Nucl. Sci.* **23** (1976) 1497.
- 24) L. C. Kimerling, M. T. Asom, J. L. Benton, P. J. Drevinsky and C. E. Cafer: *Mater. Sci. Forum* **38–41** (1989) 141.
- 25) P. M. Mooney, L. J. Cheng, M. Sili, J. D. Gerson and J. W. Corbett: *Phys. Rev. B* **15** (1977) 3836.
- 26) I. Weinberg and C. K. Swartz: *Appl. Phys. Lett.* **36** (1980) 693.
- 27) I. Weinberg, S. Mehta and C. K. Swartz: *Appl. Phys. Lett.* **44** (1984) 1071.
- 28) G. Ferenczi, C. A. Londos, T. Pavelka and M. Somogyi: *J. Appl. Phys.* **63** (1988) 183.
- 29) A. R. Frederickson, A. S. Karakashian, P. J. Drevinsky and C. E. Cafer: *J. Appl. Phys.* **65** (1989) 3272.
- 30) L. W. Song and G. D. Watkins: *Phys. Rev. B* **42** (1990) 5759.
- 31) L. W. Song, X. D. Zhan, B. W. Benson and G. D. Watkins: *Phys. Rev. B* **42** (1990) 5765.
- 32) P. J. Drevinsky, C. E. Cafer, L. C. Kimerling and J. L. Benton: in *Defect Control in Semiconductors*, ed. K. Sumino (Elsevier, Amsterdam, 1990) p. 341.
- 33) P. Nubile, J. C. Bourgoin, D. Stievenard, D. Deresmes and G. Strobl: *J. Appl. Phys.* **72** (1992) 2673.
- 34) M. Zazoui, J. C. Bourgoin, D. Stievenard, D. Deresmes and G. Strobl: *J. Appl. Phys.* **76** (1994) 815.
- 35) M.-A. Trauwert, J. Vanhellefont, H. E. Maes, A.-M. Van Bavel, G. Langouche, A. Stesmans and P. Clauws: *Mater. Sci. Eng. B* **36** (1996) 196.
- 36) D. V. Lang: *J. Appl. Phys.* **45** (1974) 3023.
- 37) D. K. Schroder: *Semiconductor Materials and Device Characterization* (Wiley, New York, 1998) 2nd ed., pp. 276 and 290.
- 38) H. Matsuura and K. Sonoi: *Jpn. J. Appl. Phys.* **35** (1996) L555.
- 39) H. Matsuura: *Jpn. J. Appl. Phys.* **36** (1997) 3541.
- 40) H. Matsuura, T. Kimoto and H. Matsunami: *Jpn. J. Appl. Phys.* **38** (1999) 4013.
- 41) H. Matsuura, Y. Masuda, Y. Chen and S. Nishino: *Jpn. J. Appl. Phys.* **39** (2000) 5069.
- 42) H. Matsuura, K. Morita, K. Nishikawa, T. Mizukoshi, M. Segawa and W. Susaki: *Jpn. J. Appl. Phys.* **41** (2002) 496.
- 43) H. Matsuura, K. Aso, S. Kagamihara, H. Iwata, T. Ishida and K. Nishikawa: *Appl. Phys. Lett.* **83** (2003) 4981.
- 44) H. Matsuura, H. Nagasawa, K. Yagi and T. Kawahara: *J. Appl. Phys.* **96** (2004) 7346.
- 45) H. Okushi: *Philos. Mag. B* **52** (1985) 33.
- 46) H. Matsuura: *J. Appl. Phys.* **64** (1988) 1964.
- 47) H. Matsuura, T. Hase, Y. Sekimoto, M. Uchida and M. Shimizu: *J. Appl. Phys.* **91** (2002) 2085.
- 48) S. M. Sze: *Physics of Semiconductor Devices* (Wiley, New York, 1981) 2nd ed., Chap. 1.
- 49) Please read the following if more precise values than those determined by FCCS are required. From FCCS, the number ( $n_{\text{species}}$ ) of acceptor species and hole traps that mainly affect  $p(T)$  is determined, which is needed to obtain the accurate densities and energy levels of acceptors and hole traps from a least-squares fit to  $p(T)$  because the values determined by the least-squares fit strongly depend on the  $n_{\text{species}}$ . From FCCS, moreover, reliable densities and energy levels of acceptors and hole traps are obtained. The most precise values can be obtained by the least-squares fit when the  $n_{\text{species}}$  is known and when the reliable densities and energy levels can be used as an initial value. As a result, the values in the text are most suitable for simulating  $p(T)$ .
- 50) N. Nagai, H. Ishida, T. Hisamatsu, T. Aburaya and S. Matsuda: *J. Cryst. Growth* **210** (2000) 74.
- 51) O. Madelung: *Semiconductors: Data Handbook* (Springer, Berlin, 2004) 3rd ed., p. 28.
- 52) G. Zoth and W. Bergholz: *J. Appl. Phys.* **67** (1990) 6764.